THE JOURNAL OF PHYSICAL CHEMISTRY B

Article

pubs.acs.org/JPCB

Surface-Enhanced Raman Scattering of Whole Human Blood, Blood Plasma, and Red Blood Cells: Cellular Processes and Bioanalytical Sensing

W. R. Premasiri,[†,‡] J. C. Lee,[§] and L. D. Ziegler*[,†,‡]

[†]Department of Chemistry, 590 Commonwealth Ave., Boston University, Boston, Massachusetts 02215, United States

[‡]Photonics Center, 15 Saint Mary's St., Boston University, Boston, Massachusetts 02215, United States

[§]Brigham and Women's Hospital, Harvard Medical School, 181 Longwood Avenue, Boston, Massachusetts 02115, United States

Supporting Information

ABSTRACT: SERS spectra of whole human blood, blood plasma, and red blood cells on Au nanoparticle SiO_2 substrates excited at 785 nm have been observed. For the sample preparation procedure employed here, the SERS spectrum of whole blood arises from the blood plasma component only. This is in contrast to the normal Raman spectrum of whole blood excited at 785 nm and open to ambient air, which is exclusively due to the scattering of oxyhemoglobin. The SERS spectrum of whole blood shows a storage time dependence that is not evident in the non-SERS Raman spectrum of whole blood. Hypoxanthine, a product of purine degradation, dominates the SERS spectrum of blood after ~10−20 h of storage at 8 °C. The corresponding SERS spectrum of plasma isolated from the stored blood shows the same temporal release of hypoxanthine. Thus, blood cellular components (red blood cells, white blood cells, and/or platelets) are releasing hypoxanthine into the plasma over this time interval. The SERS spectrum of red blood cells (RBCs) excited at 785 nm is reported for the first time and exhibits well-known heme group marker bands as well as other bands that may be attributed to cell membrane components or protein denaturation contributions. SERS, as well as normal Raman spectra, of oxy- and met-RBCs are reported and compared. These SERS results can have significant impact in the area of clinical diagnostics, blood supply management, and forensics.

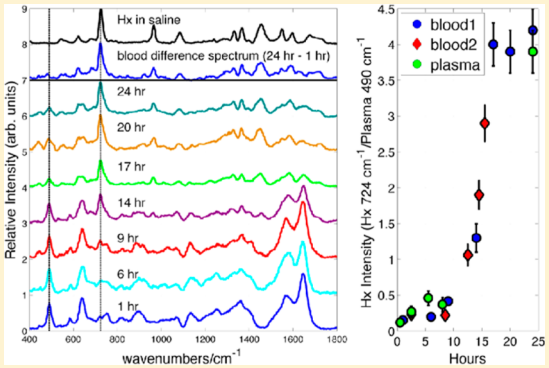

INTRODUCTION

Due to its easy access and key roles in biological activity, qualitative and quantitative chemical analysis of human blood provides a commonly used and key diagnostic for a wide variety of diseases. In addition, measures of blood components allow routine monitoring of many pathologies as well as health levels in humans more generally. A large number of analytical techniques are employed for these purposes. However, optical analytical approaches for distinguishing specific components in complex biological mixtures often offer advantages of speed, ease-of-use, and cost. Raman spectroscopy, in particular, is additionally attractive as a potential diagnostic tool because it requires no extrinsic labeling, is not limited by masking water contributions, and is inherently a multiplexing technique. Raman relies on the inherent vibrational motions as labels, resulting in specific, molecular level spectroscopic signatures, and the narrow vibrational line widths provide the ability to identify multiple components of a sample mixture from spectral analyses. Raman-based measurements of blood have already been exploited for the identification of molecular specific markers for disease detection and monitoring. For example, the use of whole blood or plasma Raman spectra for glucose level monitoring (diabetes),[1,2] cancer screening,[3−7] cardiovascular risk evaluation,[8] and detection of rheumatoid arthritis,[9] prions,[10,11] hemoglobin related blood diseases,[12] early malarial infection,[13] renal dysfunction (urea and creatine levels),[8] and other blood and serum constituents[8,14−16] have been previously described. The complete characterization of the inherent Raman properties of whole blood and its constituents, however, is required for the development of this methodology for accurate diagnostic and clinical applications. This report describes our initial efforts to exploit the well-established phenomenon of surface enhanced Raman spectroscopy[17−20] (SERS) to more carefully examine the potential for Raman spectroscopy to act as a probe of biological activity in whole human blood and to characterize the SERS features of red blood cells (RBCs), the most common type of cellular component in blood.

In SERS, Raman effective cross sections are typically enhanced by 10^6−10^8 for some normal modes of molecules in close proximity to nanostructured metal surfaces when the incident and scattering radiation is resonant with the surface

Received: May 21, 2012
Revised: June 28, 2012
Published: July 10, 2012

 © 2012 American Chemical Society

plasmon excitations of these surfaces.[17−20] The use of SERS can significantly extend the range of applicability of Raman for monitoring analytes in complex biological samples by offering advantages of sensitivity and specificity over normal spontaneous Raman. The large Raman enhancement factor offers the potential for SERS to be used to detect and identify low concentration blood constituents which may be difficult to discern via normal Raman scattering. Second, the distance and orientation dependence of the SERS enhancement mechanisms could allow access to vibrational modes not readily observed in normal Raman spectra, thus enhancing the structural information available via inelastic light scattering.[17,20,21] The consequent appearance of vibrational bands that may be weak or missing from normal or resonance Raman spectra of a species may, however, also be a liability especially for complex biological structures in terms of making vibrational assignments. In addition, small vibrational frequency shifts often observed in SERS, resulting from proximity to the SERS active surface,[22,23] can also complicate vibrational band assignments in biological macromolecules. These advantages and complications are illustrated in this SERS study of whole blood, blood plasma, and RBCs.

Despite the extensive interest in exploiting SERS for a wide variety of bioanalytical applications and the central biological role of blood, there have been no prior 785 nm excited SERS studies of whole human blood. Only a SERS study of whole blood mixed with Ag colloid excited at 514.5 nm has recently appeared.[24] A few bands associated with the heme group were identified. To the best of our knowledge, only a single previous SERS study of RBCs has been previously reported as well.[25] In that study, SERS spectra of RBCs mixed with Ag colloids appeared to indicate a submembrane hemoglobin population as distinct from the cytoplasmic population which dominates the 532 nm excited near resonance Raman spectrum of hemoglobin.

Several investigators have used SERS, however, for the study of disease markers in human serum, including measurements obtained with 785 nm excitation.[3−6,16,26,27] The data reported here are crucial to understanding the biological significance of results described in those papers as shown below. A few SERS studies of hemoglobin, including one recent report at 785 nm,[28] have been given and discussed in the context of the denaturing effect of metal nanostructured surfaces,[29] single molecule spectroscopy,[30] and sensitive hemoglobin detection.[28] The convenient accessibility of hemoglobin electronic transitions for excitation by readily available commercial visible laser frequencies probably lessened the perceived need for SERS studies of whole blood, RBCs, and hemoglobin. However, as shown here, SERS provides an alternative and complementary approach for learning about such heme containing samples and Raman-based biomedical applications more generally.

Aside from the medical applications highlighted above, exploiting SERS for blood analysis could also impact other fields. Recently, Raman analysis of body fluids, including blood, has been shown to be of potential value for forensic purposes, allowing nondestructive, rapid, on-site identification of human body fluids.[31,32] Thus, the continuing characterization of the Raman activity of human blood and its components may have potential importance additionally in the developing area of forensic science.

Our research group has recent and ongoing efforts to develop a SERS-based platform for a rapid bacteremia diagnostic. *In vitro* cultured bacterial cells placed on a novel, *in situ* grown, Au nanoparticle covered SiO_2 SERS active substrate,[33] yield reproducible, high quality characteristic spectral signatures that can be used for bacterial identification when combined with a unique multivariate data analysis approach.[34,35] SERS spectra of bacteria have also been observed from enriched bacteria-spiked blood samples,[36] and efforts are continuing to further develop this protocol.[37] However, in developing a SERS based platform for a diagnostic of bacteria enriched from human blood samples, an understanding and characterization of the SERS signals due to whole blood components that may remain after the enrichment process is required and is an additional motivation for these studies.

Thus, the SERS spectra of 785 nm excited whole human blood, blood plasma, and its major cellular constituent, RBCs, on Au nanoparticle covered SiO_2 substrates[33] are reported here. The time dependence of these signals, and their comparison with non-SERS spectra and previous reports, are considered in detail. The results suggest some novel applications for SERS spectroscopy of whole blood and its components.

■ EXPERIMENTAL SECTION

Sample Preparations. Following standard protocols, 5 mL of blood was collected by venipuncture from healthy donors into vacutainer blood collection tubes containing EDTA as an anticoagulant (BD, Franklin Lakes, NJ). Samples were stored in an 8 °C refrigerator until required for measurements or additional separation steps. Blood plasma was separated from the blood by centrifugation at 10 000 rpm for 2 min. RBCs were obtained via a gradient centrifugation procedure. 5 mL of human peripheral venous blood with EDTA was layered on 5 mL of polymorphprep liquid (Accurate Chemical and Scientific Corp.) in a 15 mL polypropylene tube. The sample was centrifuged at 450*g* using an Eppendorf 5804R centrifuge at 18 °C. All the liquid above the RBC pellet was discarded. The RBC pellet was resuspended in a normal saline solution and washed four times with saline solutions prior to use.

MetRBCs were prepared from a centrifugation (1 min at 10 000 rpm) concentrated RBC sample.[38] 10 μL of concentrated RBCs was suspended in 10 mL of 0.1 wt % sodium nitrite in PBS (phosphate buffered saline) and incubated for 1 h at room temperature. MetRBCs were recovered after centrifugation and washed three times with saline before resuspending in 0.5 mL of saline for data acquisition.

SERS Spectral Data Acquisition. All the SERS spectra reported here were acquired on substrates resulting from an *in situ* Au ion doped SiO_2 sol−gel procedure previously developed in our laboratory.[33] This procedure results in small (2−15 particles) aggregates of monodispersed ∼80 nm Au nanoparticles covering the outer layer of ∼1 mm^2 SiO_2 substrate. An SEM image of this chemically produced substrate is shown in the Supporting Information (Figure S1). The sol−gel based process was maximized for optimal 785 nm excited SERS performance and exhibits a broad surface plasmon resonance centered at ∼800 nm. Extensive details concerning the production of these SERS active chips and the characterization of their performance for providing reproducible and strongly enhanced (single cell level) SERS spectra of bacteria when excited by a few milliwatts of 785 nm radiation have been previously described.[33]

An RM-2000 Renishaw Raman microscope employing either a 50× or 20× objective and 785 nm excitation was used to obtained all of the spectra shown here. SERS spectra typically resulted from <2 mW of incident laser power in ∼10 s of

illumination time. The 520 cm^{-1} band of a silicon wafer was used for frequency calibration.

RESULTS AND DISCUSSION

Whole Human Blood. *Normal Raman Spectra.* Raman spectra of whole human blood excited at 785 nm are shown in Figure 1 for two different methods of sample preparation.

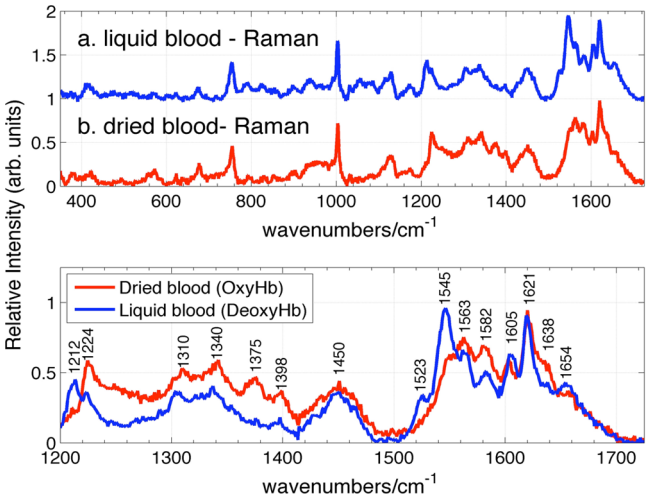

Figure 1. Normal (non-SERS) Raman spectra excited at 785 nm of (a) liquid whole blood in sealed cuvette and (b) dried whole blood sample are shown in upper panel. Frequencies of liquid and dried blood sample corresponding to deoxy- and oxyhemoglobin respectively are shown in the lower panel.

These normal (non-SERS) Raman spectra are reported here to allow a comparison with the corresponding, subsequently described 785 nm excited SERS spectra of whole blood. The Raman spectrum of a human blood sample, collected 30 min prior to data acquisition and placed in a capped quartz tube to prevent clotting, is the (blue) spectrum, labeled *a*, in the upper panel of Figure 1. The Raman spectrum labeled *b* in the same panel of Figure 1 results from a drop of blood that has been placed on a silicon wafer, open to the ambient air and allowed to dry for about 1 h. 1.8 mW of incident laser power and 20 s data accumulation times are used to acquire these non-SERS Raman spectra. As evident in Figure 1, there is a close correspondence between the pattern of relative vibrational intensities and frequencies observed in these two 785 nm excited non-SERS Raman spectra of whole human blood. However, small spectral shifts and relative intensity changes are evident for some vibrational features when the liquid (a) and dried blood (b) Raman spectra are compared in greater detail. For example, as seen in the lower panel of Figure 1, where these spectra are compared in greater detail in the 1200−1750 cm^{-1} region, vibrational band peaks at 1523, 1545, and 1605 cm^{-1} are more prominent in the liquid spectrum, whereas 1563, 1582, and 1638 cm^{-1} bands are relatively stronger in the dried blood spectrum. The relative intensities of the 1212 and 1224 cm^{-1} bands change in the dried and liquid blood spectra, bands at 1374 and 1398 cm^{-1} are much stronger in the dried blood spectrum, and a number of other bands exhibit small but measurable frequency shifts when these two spectra are carefully compared.

The observed vibrational features in the Raman spectra of whole blood excited by radiation in the 720−830 nm range reported previously have been variously attributed to blood proteins[24,31,32] and other known blood constituents[14,15] (glucose, urea, cholesterol, triglycerides), in addition to hemoglobin. However, based on previous Raman studies of RBCs and hemoglobin excited at 785 nm or in the NIR, all the observed blood bands (Figure 1) can be assigned to normal modes of either the oxygenated or deoxygenated hemoglobin porphyrin macrocycle and hemoglobin protein constituents.[39−44] The observed Raman vibrational frequencies of liquid and dried whole human blood (Figure 1) and their corresponding vibrational assignments are summarized in Table 1. The vibrational bands observed in this normal Raman spectrum are nearly identical to the previously reported non-SERS spectra of whole human blood excited by near-IR

Table 1. Observed Vibrational Bands of "Normal" (Non-SERS) Raman Spectrum of Whole Human Blood (Liquid Drop and Dried Blood) at 785 nm

observed band[b] (cm^{-1})	intensity	assignment[a]	observed band[b] (cm^{-1})	intensity	assignment[a]
347[d]	m	ν_8	1127,[d] 1129[e]	m	ν_5
380[d]	w	$\delta(C_\beta C_c C_d)$	1173	w	ν_{30}
417	m	δ(Fe−O−O)	1212[e]	m	$\nu_5 + \nu_{18}$
570	w	$\nu(Fe-O_2)$	1224	w,[e] m[d]	ν_{13} or ν_{42}
621	w	ν_{12}	1305,[e] 1311[d]	w	ν_{21}
674,[e] 677[d]	m	ν_7	1338,[e] 1341	m	ν_{41}
716	w	γ_{11}	1374,[d] 1377[e]	m,[d] vw[e]	ν_4
754	s	ν_{15}	1398	m	ν_{20}
788	w	ν_6	1450	s	$\delta(CH_2/CH_3)$
825[e]	w	γ_{10}	1523[e]	m	ν_{38}
856	w		1545[e]	s	ν_{11}
900	w	p: C−C skeletal	1563	s	ν_{19}
937	m	ν_{46}	1582	m	ν_{37}
1003	s	phenylalanine	1605[e]/03[d]	m	$\nu(C_a{=}C_b)$
1030	w	$\delta(=C_bH_2)_{asym}$	1621	s	$\nu(C_a{=}C_b)$
1054	w	$\delta(=C_bH_2)_{asym}$	1638	m,[d] w[e]	ν_{10}
1115[e]	w		1654	w	amide I

[a]Assignments based on refs 39, 43, and 69. p = protein. C_α, C_β, and C_m represent the carbon atoms at the alpha, beta, and meso positions of porphyrins, respectively; C_a and C_b are vinyl group carbons. [b]Estimated precision ±1 cm^{-1}. [d]Dried blood sample. [e]Liquid blood sample.

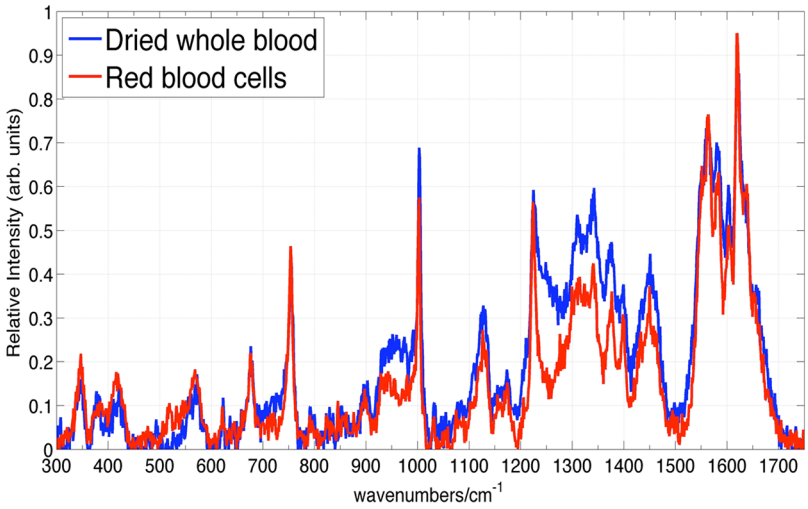

Figure 2. The 785 nm excited Raman spectrum of dried whole blood and RBCs.

radiation (720 or 830 nm).[14,31,42,45] Furthermore, comparison with previous Raman studies of oxygenated and deoxygenated single RBCs[39] and hemoglobin[40] reveals that the most significant differences between the dried and liquid whole blood Raman spectra excited at 785 nm (Figure 1) are due to the state of hemoglobin oxygenation. Marker bands associated with oxygenated hemoglobin dominate the dried blood spectrum, and those of deoxygenated hemoglobin dominate the fresh liquid blood spectrum.[39,40] The predominance of deoxygenated hemoglobin for the liquid hemoglobin sample liquid is due to the venous source of this blood sample collected in a vacuum sealed tube, hence limiting its contact with ambient air. The dried blood sample, in contrast, has been open to the ambient air for at least 60 min before data acquisition which is sufficient time for oxygen binding.[9]

Further evidence that the 785 nm excited non-SERS Raman spectrum of whole blood is exclusively due to hemoglobin is provided by a comparison of the Raman spectra of dried whole blood and ambient exposed (oxygenated) RBCs at this excitation wavelength. The 785 nm excited Raman spectrum of whole blood is virtually identical to that of RBCs as shown in Figure 2. Thus, in agreement with Sato et al.,[42] we find that the 785 nm excited whole blood Raman spectrum is derived exclusively from the hemoglobin of RBCs and gives no information about the other components of this complex inhomogeneous biological mixture.

Finally, we note that it is essential to keep incident Raman excitation fluence and total illumination energy at low levels ($<7 \times 10^4$ W/cm^2 and less than 30 s data collection time) in order to avoid contributions due to photothermal and photochemical effects in the Raman spectra of whole blood. Above these excitation power levels at 785 nm, fluence-dependent Raman spectra, including a broad fluorescence-like emission background, are observed with characteristic new vibrational frequencies due to denaturation and hemoglobin aggregation as previously reported for RBCs.[39,41] This fluence dependence may contribute to some of the variability seen in the previously reported spectra of whole blood.[14,15,31]

SERS Spectrum. The SERS spectrum of fresh whole human blood excited at 785 nm is shown in Figure 3b. The freshly drawn blood sample was refrigerated (8 °C) prior to SERS measurements. ~1 μL of this blood sample was placed on the Au SERS substrate,[33] and as much of this sample volume as possible was removed immediately with a pipet leaving only a thin film of blood on the SERS active surface. A SERS spectrum was acquired after the sample was allowed to completely dry (~5 min). In contrast to the normal Raman spectrum of whole blood (Figure 3a) excited with ~2 mW for 20 s (20× objective, average of five spectra), the SERS spectrum (Figure 3b) results from 10 s of 0.45 mW incident 785 nm laser power (50× objective, single scan). In this fresh blood sample, observed ~1 h after being drawn, strong vibrational transitions are observed at 490, 639, 895, 1134, 1362, 1569, and 1649 cm^{-1} in the SERS spectrum (Figure 3b). The observed vibrational frequencies of the bands in this SERS spectrum of whole blood are indicated on the displayed SERS spectrum (Figure 3b). Comparison of the SERS spectrum of whole blood (Figure 3b) with the normal Raman spectrum excited at 785 nm (Figure 3a) reveals that there are virtually no vibrational bands that appear in both of these spectra. Thus, the SERS spectrum of whole human blood excited at 785 nm is due to blood components *other than* hemoglobin. This is in dramatic contrast to the normal Raman spectrum of whole blood excited at 785 nm, which is exclusively due to hemoglobin, as discussed above.

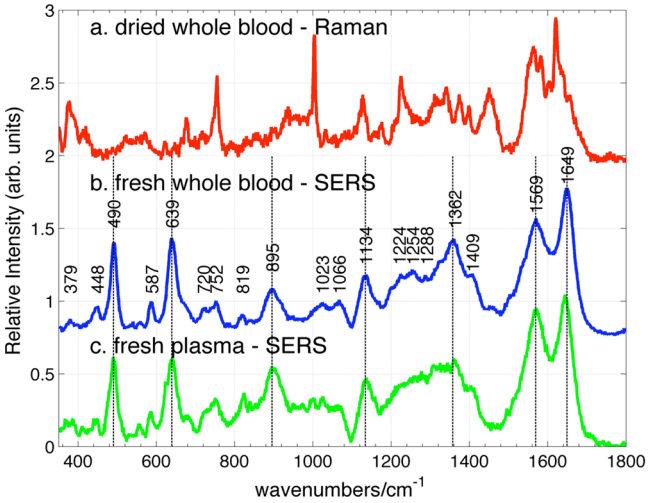

Figure 3. The 785 nm excited (b) SERS spectrum of fresh whole blood compared to (a) normal Raman spectrum of dried whole blood and (c) SERS spectrum of fresh plasma. The peak positions of the bands in the SERS spectrum of fresh whole blood are given in (b).

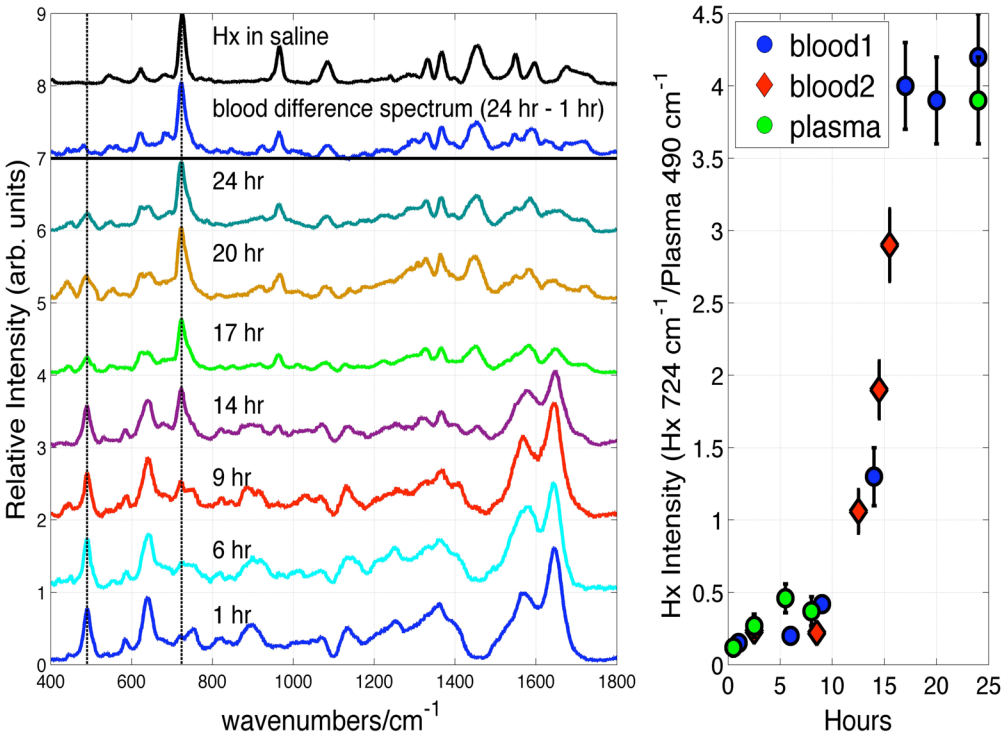

Figure 4. SERS spectrum of whole blood as a function of storage time (4 °C), 24 h−1 h SERS blood difference spectrum, and the SERS spectrum of hypoxanthine (Hx) in normal saline solution are shown in the left-hand panel. The relative intensities of the time-dependent whole blood SERS spectra have been normalized by the observed signal size intensity of the largest feature in the 24 h spectrum at 724 cm^{-1}. The SERS intensity of the 724 cm^{-1} band of Hx relative to the 490 cm^{-1} band of whole blood, and the 724 cm^{-1} band of Hx relative to the 490 cm^{-1} band of a blood plasma sample as a function of storage time are shown in the right-hand panel.

Although no prior reports of 785 nm excited SERS spectra of fresh whole blood have appeared, a SERS spectrum of whole blood excited at 514.5 nm, resulting from mixing blood with a Ag colloid solution, has been recently published.[24] Only a few vibrational bands are evident in that spectrum, and they are attributed to hemoglobin, in contrast to the 785 nm SERS results presented here (Figure 3b). Only two of the 785 nm SERS bands of whole blood (1649 and 1569 cm^{-1}) appear to correspond to features seen in the 514.5 nm SERS spectrum (1640 and 1587 cm^{-1}). The blood components accounting for this SERS spectrum of whole blood excited at 785 nm are discussed further below.

A key observation central to the use of SERS of whole blood for bioanalytical and diagnostic applications is illustrated in Figure 4. In the left-hand panel, the SERS spectra of the same blood sample stored at 8 °C are shown as a function of storage time over a period of 24 h. For display purposes, these spectra have been normalized by the intensity of the largest feature in the 24 h spectrum at 724 cm^{-1}. As seen in Figure 4, the 785 nm excited SERS spectrum of whole blood dramatically changes over this time frame. For example, new vibrational bands appear at 724, 965, 1070, 1332, 1365, and 1453 cm^{-1} and increase in relative importance as a function of whole blood storage time. The 24 h minus the 1 h difference SERS spectrum of whole blood is shown in the top part of this Figure 4 panel. This difference spectrum is compared to the SERS spectrum of hypoxanthine, a well-known purine degradation product, in normal saline solution (0.9 wt % NaCl) in this figure as well. All the major bands of this whole blood difference spectrum correspond in frequency and relative intensity to the SERS spectrum of hypoxanthine. Furthermore, the SERS spectrum of whole blood stored for ∼24 h is essentially that of hypoxanthine. The 490 cm^{-1} vibrational band is a strong Raman feature of the SERS spectrum of fresh whole blood (Figures 3b and 4) and thus can be used as an internal standard for the changes in relative intensity as a function of time. Vertical lines at 490 and 724 cm^{-1} in Figure 4 highlight the changes in relative intensities of these two components over the ∼24 h time period. In the panel on the right-hand side of Figure 4, the intensity of the 724 cm^{-1} band of hypoxanthine relative to the 490 cm^{-1} transition of the fresh whole blood spectrum is plotted as a function of time. As seen in this figure, the time dependence of the hypoxanthine signal is not linear with time, and its concentration dramatically increases after ∼15 h of storage. The hypoxanthine signal appears to saturate after ∼24 h, when it is found to completely dominate the 785 nm SERS spectrum of whole blood. In this limited blood sampling, the hypoxanthine concentration in whole blood increases by ∼50−100 times its value in fresh blood and reaches a maximum value of ∼200 μM, for the blood of the donor followed for the ∼24 h period. This concentration estimate is calibrated by the SERS intensities of hypoxanthine in fresh blood plasma solutions of known concentrations. The time profile of the hypoxanthine signal (Figure 4) is potentially donor dependent, as well as donor history dependent for a single donor, and will be the subject of future investigations.

Aside from revealing that SERS can be a sensitive probe of biological activity in this complex body fluid, and offering a potential means for understanding the fundamental biochemical processes that account for this time dependent hypoxanthine signal, the data in Figure 4 highlight the potential difficulties that can be encountered when trying to develop SERS-based whole blood assays for disease detection and identification due to the "age" of the blood sample alone. The

inherent SERS signature of whole blood is *time-dependent*. This is a complication for the use of whole blood SERS for bioanalytical investigations if fresh blood samples are not used immediately (within ~1 h). In order to further understand the origin and time-dependent characteristics of the SERS spectra of human whole blood, a SERS study of all the readily separated constituents of blood is necessary. Here we report in detail only on the temporal evolution of the SERS spectrum of blood plasma. It is important to emphasize that no hypoxanthine bands are evident in the normal, i.e., non-SERS, spectrum of whole blood during this 24 h period (not shown).

Blood Plasma. Approximately 1 μL of blood plasma, the resulting clear yellow supernatant corresponding to the nonparticulate liquid component of anticoagulated blood, was placed on the Au nanoparticle covered SERS substrate. SERS spectra of blood plasma were obtained after waiting ~5 min to allow reduction of the sample volume due to water evaporation. A 785 nm excited SERS spectrum of plasma derived from a fresh blood sample (~1 h after being drawn) is shown in Figure 3c. The SERS spectrum of plasma resulting from our Au nanoparticle covered SiO_2 "chips" (Figure 3c) exhibits similar vibrational frequencies as reported for the SERS spectra of plasma due to other plasmonically enhancing substrates excited at 785 nm, including enriched Au[5] and Ag[3,4,6,26] colloid solutions and a PVA–Ag nanoparticle films.[27] As seen in Figure 3, the SERS spectrum of fresh whole blood (Figure 3b), prepared as described above on our SERS substrate, is virtually identical to that of fresh plasma (Figure 3c). The pattern of relative band intensities and frequencies are the same in both spectra. Vertical lines in Figure 3 highlight the correspondence between the features in these two SERS spectra (and their absence in the normal Raman spectrum of whole blood). Thus, the 785 nm excited SERS spectrum of fresh whole blood, resulting from the sample preparation procedure employed here, is dominated by the plasma component of whole blood. When a thin layer of blood is placed on our nanostructured Au surface, no significant vibrational features arising from RBCs, white blood cells (mononuclear or polymorphonuclear cells), or platelets are evident in the whole blood SERS spectrum at this excitation wavelength. The SERS spectrum of fresh blood plasma must arise from the wide variety of components that make up this aqueous solution: proteins (albumins, globulins, fibrinogen, hormones), lipoproteins (protein complexes with cholesterol, phospholipids, triglycerides), carbohydrates (glucose), other small organic molecules (vitamins, steroids, amino acids, nucleic acids), and metabolites excreted by the cells. A detailed vibrational assignment of the chemical origins of the observed features of the reported 785 nm SERS spectrum of fresh human blood plasma, and hence that of fresh whole blood, is outside of the scope of this study and will be addressed in subsequent work.

Further confirmation that the whole blood SERS spectrum is just that of blood plasma and some initial insight into the origin of the time dependent hypoxanthine contribution to the SERS spectrum of whole blood is derived from the time dependence of the SERS plasma signals. The 785 nm excited SERS spectra of plasma as a function of blood storage time are displayed in Figure 5. This time corresponds to the age of the stored whole blood when the plasma was removed via centrifugation from the whole blood sample and then immediately placed on the SERS substrate for signal acquisition, as described above. The relative intensities of these spectra are normalized to the value of the peak signal size of the 724 cm^{-1} band at 24 h. As shown

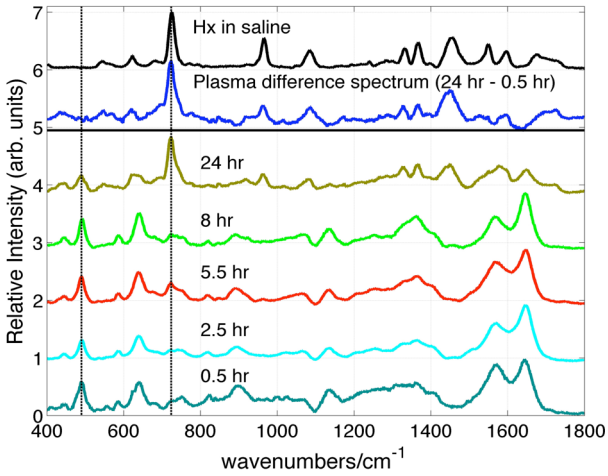

Figure 5. SERS spectra of the plasma derived from stored (8 °C) blood as a function of storage time compared with the SERS spectrum of hypoxanthine (x μM) in normal saline solution. The 24 h–0.5 h SERS difference spectrum of stored blood plasma is also shown.

in Figure 5, this feature is the strongest band in the 785 nm excited SERS spectrum of hypoxanthine. Just as is found for the whole blood spectrum (Figure 4), hypoxanthine appears in the SERS spectrum of plasma (Figure 5) over a period of ~24 h with a rate that appears nearly identical to that seen for the whole blood samples (Figure 4, right panel). The 24 h–0.5 h SERS difference spectrum of plasma is found to be identical with the SERS spectrum of hypoxanthine (Figure 5), and the 785 nm excited SERS spectrum of plasma separated from blood stored for ~24 h is dominated by the spectrum of hypoxanthine. The SERS spectrum of plasma separated from fresh blood and stored independently displays only a very minimal increase in hypoxanthine concentration over this same time frame. Thus, the increasing concentration of hypoxanthine observed in the whole blood spectrum as a function of time (Figure 4) corresponds to the leakage of this species into the extracellular fluid from one or more cellular components during this time frame. Knowledge of the time dependence of the hypoxanthine contribution to the SERS of whole blood and plasma is essential for the development of a plasma or whole blood based SERS diagnostic.

Erythrocytes/RBCs. Erythrocytes or RBCs, primarily responsible for delivering O_2 throughout the body, are the most abundant cells in humans and are present in blood at concentrations of (4–6) × 10^9/mL. They are flexible biconcave disks that are 6–8 μm in diameter and 2 μm thick. The ratio of RBCs to white blood cells to platelets in human blood is approximately 600:1:40. Furthermore, about 33% of RBCs are hemoglobin by volume. As discussed above, the Raman spectrum of RBCs and dried whole blood excited at 785 nm (Figure 2) is dominated by oxygenated hemoglobin vibrational modes. While a few modes attributable to the non-porphyrin-related component of the hemoglobin protein are evident, such as the amide I (1654 cm^{-1}), phenylalanine ring stretching (1003 cm^{-1}), and CH_2/CH_3 amino acid deformation modes (1450 cm^{-1}), most of the vibrational features are due to the Raman activity of the heme porphyrin moiety in the non-SERS spectrum (Figure 2). RBCs are a convenient target for Raman studies owing to the well-known visible electronic transitions of the heme group,[46] allowing resonance Raman access to the structural sensitive vibrational spectrum.[47] The strong Soret

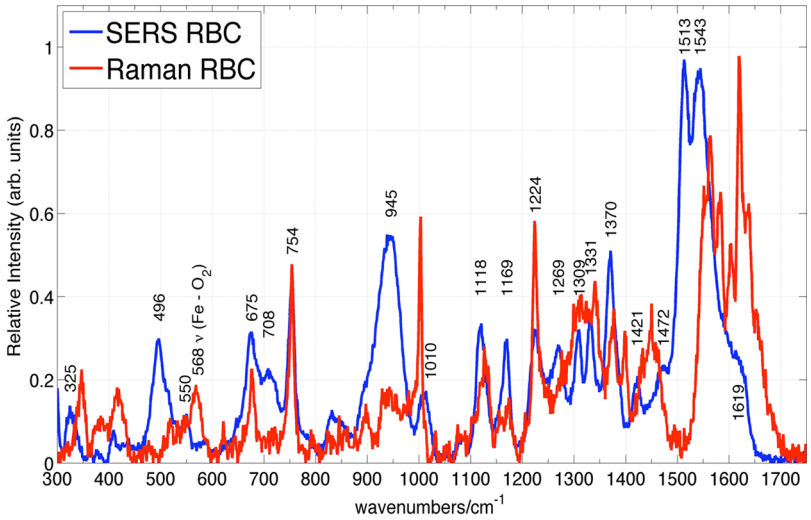

Figure 6. Comparison of SERS and normal Raman spectra of RBCs excited at 785 nm. The observed frequencies and tentative assignment of the RBC SERS vibrational bands are indicated.

(405−430 nm, $\varepsilon \sim (1.3-1.9) \times 10^5$ M^{-1} cm^{-1}) and weaker $\alpha-\beta$ band (or Q-band) (500−600 nm, $\varepsilon \sim 1.0 \times 10^4$ M^{-1} cm^{-1}) transitions are significantly blue-shifted from 785 nm, and hence the spectra reported and discussed here are, at best, in the preresonant region. A weak charge transfer excitation centered at ∼760 nm ($\varepsilon \sim 300$ M^{-1} cm^{-1}) has been identified for deoxyhemoglobin,[48] but that species does not appear to be significantly present in these ambient air exposed blood and RBC samples. The 785 nm excited Raman spectrum of RBCs (Figures 2 and 6) are in agreement with those previously reported for oxygenated RBCs at this excitation wavelength,[39,43,49,50] as noted above.

The corresponding SERS spectrum of RBCs isolated from fresh whole blood is shown in Figure 6 and overlapped with the normal Raman spectrum of RBCs excited at 785 nm. To the best of our knowledge, this is the first nonelectronically resonant SERS spectrum of RBCs. In fact, only one prior SERS spectrum of RBCs, obtained with excitation at 532 nm, resulting from a red blood cell mixture with Ag colloids, has been reported.[25] This visible excitation wavelength is resonant with the Q-band region, and thus, the intensities of these vibrational bands, which are also attributed to oxygenated hemoglobin, are both electronically and plasmonically enhanced. Some vibrational bands appear in both SERS spectra; however, a few very significant differences are evident, as well, between the spectrum reported for 532 nm excitation[25] and the 785 nm one reported here (Figure 6).

As evident in Figure 6, SERS spectra of red blood cells excited at this nonresonant excitation wavelength are readily attainable with excellent signal-to-noise. The Raman illumination region (∼2.5 μm × 15 μm) for the 50× objective used in these studies is approximately equal to the area of a single red blood cell; thus, these SERS spectra (Figure 6) are at the single cell level. The enhancement factor for the Raman intensities on the Au substrates employed in these studies can be estimated for the 754 cm^{-1} band, which is a Raman feature due to the heme group (ν_{15}) observed in both the SERS and normal Raman spectrum of RBCs. When the absolute signal size is normalized for the different incident laser powers, data accumulation times, and number of cells in the scattering volume (1 vs 20), an enhancement factor of 1.2×10^3 per red blood cell is obtained for the 754 cm^{-1} mode. However, the number of hemoglobin molecules that contribute to the bulk Raman and SERS spectra per cell are quite different. Because of the distance dependence of the SERS enhancement mechanisms, only those molecules that are close (<∼5 nm) to the nanostructured metal surface will be plasmonically enhanced. Approximately 0.5% of the hemoglobins are estimated to be bound at the inner surface of the red blood cell membrane,[25,51,52] and furthermore, if we estimate that ∼40% of the entire cell surface is in close contact with the nanostructured metal surface, then the SERS enhancement factor (EF) is $\sim 10^6$ per hemoglobin. This EF value is lower than what we usually achieve on these SERS substrates (10^7−10^8)[33] but is consistent with the location of the submembrane hemoglobin population at a distance of ∼4−5 nm from the extracellular edge of the red blood.[25,51]

The vibrational frequencies of the bands observed in the 785 nm excited normal Raman and SERS spectra of RBCs (Figure 6) are listed in Table 2. Vibrational frequencies for some transitions are unchanged in these SERS and normal Raman spectra of RBCs: 754 cm^{-1} (ν_{15}), 675 cm^{-1} (ν_7), 1224 cm^{-1} (ν_{42}/ν_{13}), whereas several appear to red-shift in the SERS spectrum: 1375 to 1371 cm^{-1} (ν_4), 1127 to 1120 cm^{-1} (ν_5), 1173 to 1169 cm^{-1} (ν_{30}), 1340 to 1332 cm^{-1} (ν_{41}), and 1551 to 1543 cm^{-1} (ν_{11}). Other vibrational bands seen in the 785 nm Raman spectrum of RBCs are not evident in the corresponding SERS spectrum: 1654 cm^{-1} (amide I), 1450 cm^{-1} (CH_2/CH_3 amino acid deformation modes), 1399 cm^{-1} (ν_{20}), and 568 cm^{-1} (ν Fe−O_2), and a few new bands, whose parentage is unclear, appear prominently in the SERS spectrum, for example bands at 1513, 551, 1471, and 496 cm^{-1}. Interestingly, the Fe−O_2 stretch mode at 568 cm^{-1} is either completely missing in the SERS spectrum or this band is significantly red-shifted perhaps corresponding to the relatively weaker band at 550 cm^{-1} or to the new strong feature at 496 cm^{-1} in the SERS red blood cell spectrum (Figure 6).

We considered the possibility that the proximity to the Au nanostructured surface could induce the transition of hemoglobins in the oxyRBCs to methemoglobin, the high-spin ferric heme protein where water takes the place of the dioxygen site.[38,53−55] The Raman and SERS spectra of oxy- and met-RBCs are shown in Figure 7, and the corresponding observed vibrational band frequencies and assignments are

Table 2. Observed 785 nm Excited Raman and SERS Bands of OxyRBCs and MetRBCs

oxyRBC[b] (cm^{-1})	metRBC (cm^{-1})	SERS oxyRBC (cm^{-1})	SERS metRBC (cm^{-1})	tentative assignt[a]
		328	328	
346	347			ν_8
382	377	380	377	$\delta(C_\beta C_c C_d)$
		408	408	$\delta(C_\beta C_a C_b)_4$ + $\delta(C_\beta Me)$
418				ν_{21} δ(Fe−O−O)
		496	497	γ_{12}
		551		ν_{49} or $\nu(Fe-O_2)$?
568				$\nu(Fe-O_2)$
		586	586	ν_{48}
621	622	621	621	ν_{12}
675	676	675	674	ν_7
715	715	710	710	ν_{11}
754	756	754	756	ν_{15}
		832	835	
897	897			
939	939	944	939	ν_{46}
1003	1003			phe
		1010	1010	ν_{45}
1031	1031			$\delta(=C_bH_2)_{asym}$
1127	1127	1120	1119	ν_5
1158				ν_{44}
1173	1174	1169	1170	ν_{30}
1210	1213			$\nu_5 + \nu_{18}$ or ν_{13}
1224	1224	1224	1228	ν_{13} or ν_{42}
		1270	1274	
1309	1309	1309	1309	ν_{21}
1340	1340	1332	1331	ν_{41}
1375	1372	1371	1371	ν_4
1399				ν_{20}
		1422	1422	ν_{28}
1450	1450			$\delta(CH_2/CH_3)$
		1471		
		1513	1515	
1551	1545	1543	1539/1547	ν_{11}
1563	1563			ν_{19}
1582	1582			ν_{37}
1603	1603			$\nu(C{=}C)_{vinyl}$
1620	1621	1620	1620	$\nu(C{=}C)_{vinyl}$
	1630		1629	
1638				ν_{10}
1654	1654			amide I

[a]Based on refs 38, 43, and 70. [b]Estimated precision ±1 cm^{-1}.

summarized in Table 2. The differences between the normal Raman spectra of oxyRBCs and metRBCs excited at 785 nm is more noticeable than between the SERS spectra of these two cells (Figure 7). However, reproducible small differences between the oxy and met RBCs SERS spectra are found, such as a distinct 1629 cm^{-1} band in metRBC spectrum which is missing in the oxyRBC spectrum, 551 and 1471 cm^{-1} bands in the oxyRBC spectrum that are not evident in metRBC spectrum, structure in the 1539−1547 cm^{-1} region of metRBC which is absent in the corresponding oxyRBC spectrum, and other small spectral shifts listed in Table 2. Thus, methemoglobin does not appear to be the species responsible for the SERS spectra of RBCs reported here.

As discussed above, SERS spectra can exhibit changes in relative vibrational intensities and small vibrational frequency shifts compared to normal Raman spectra at the same excitation wavelength owing to metal surface interactions and the orientation and distance dependence of the SERS enhancement mechanisms. Such effects appear to be affecting the SERS spectrum of RBCs reported here. In addition, new vibrational bands or frequency shifted bands may appear as a result of chemical reactivity facilitated by the proximity to the SERS active metal surface. In a prior study, the Soret band resonant SERS spectrum of oxygenated hemoglobin in a Ag colloidal solution exhibited vibrational bands assigned to the formation of surface bound hemin μ-oxo dimers.[29] Thus, heme proteins may be denatured by adsorption to the metal surface, at least under conditions of electronic resonance. Whether denaturation is responsible for the spectral changes in the SERS observed here in these nonresonant excitation conditions for the heme chromophore in the red blood cell environment will be further investigated by studies of the heme chromophore alone in these excitation condition on the Au SERS active surfaces used here and in Ag colloids. Furthermore, for intact RBCs, hemoglobin is located ∼4−5 nm from the outer layer,[25,51,52] presumably reducing the potential for the heme moiety to leave the surrounding protein and aggregate at the metal surface, as noted above in the electronically resonant hemoglobin SERS study.[29] SERS bands of RBCs tend to be broader than their corresponding vibrational transitions in the normal Raman spectrum (Figure 6). This may be attributable to a number of effects resulting from the interaction with the nanostructure metal surface, including a large inhomogeneous distribution of interaction strengths with the surface, enhanced vibrational dephasing rates, or enhanced contributions of low-frequency protein modes arising from local heating effects. Previously identified characteristic heme aggregation marker bands[39,41] (1248, 973 cm^{-1}) discussed above are not evident in the observed SERS spectra of RBCs (Figure 6), thus eliminating this potential non-native heme-based contribution to these SERS spectra.

One possible origin for the SERS vibrational bands without obvious heme parentage in the 785 nm SERS spectrum of RBCs (Figure 6), e.g. 1513, 1010, 945, or 496 cm^{-1}, are the protein, lipid, or carbohydrate components of the red blood cell membrane. Judging by the microscopic images obtained simultaneously with the SERS acquisition, these SERS spectra appear to result from intact erythrocytes. Thus, it is at least plausible that the red cell membrane components (glycoproteins, glycolipids, spectrin, cholesterol, phospholipids, transmembrane proteins, etc.), which must be closer to the SERS active surface than the hemoglobins, will contribute to these SERS spectra. Subsequent SERS studies of red blood cell ghosts and model compounds will further explore this possible origin of the "new" vibrational features in the red blood cell SERS spectra reported here.

In the one previous SERS spectrum of RBCs,[25] resulting from Q-band resonant 532 nm excitation of erythrocytes mixed with Ag colloids, small frequency shifts were observed for selected bands, relative intensities are significantly altered, and a few new bands are observed in the SERS spectrum although these are not commented on in that report. These observations are similar to the qualitative features that distinguish the 785 nm SERS and non-SERS spectra reported here. However, the pattern of relative intensities at these two excitation frequencies cannot be directly compared due to the resonant excitation

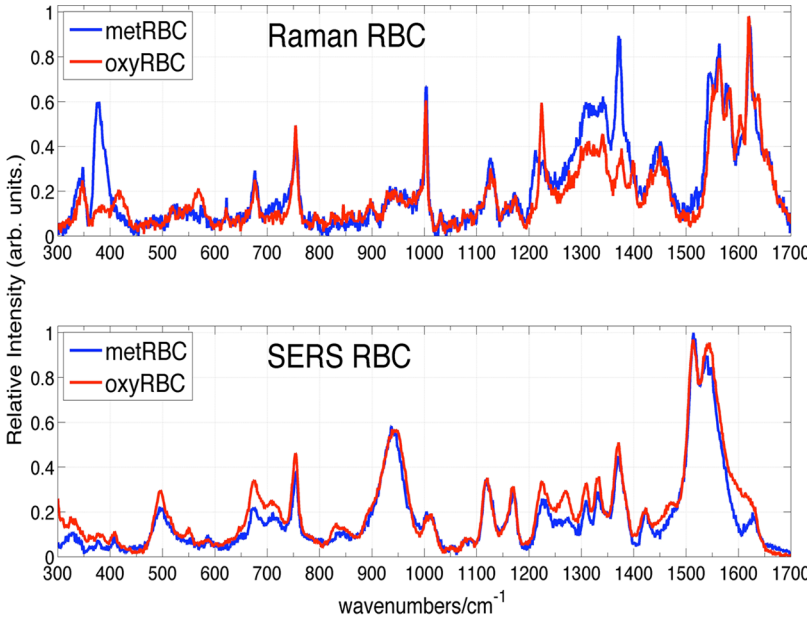

Figure 7. Normal Raman spectra of oxyRBCs and metRBCs excited at 785 nm are compared in the upper panel. The SERS spectra of oxy- and metRBCs excited at this same wavelength are compared in the lower panel.

condition of the 532 nm radiation as compared to the nonresonant 785 nm excitation. In the 532 nm study, RBCs mixed with Ag nanoparticles exhibited no change in membrane fluidity, indicating the integrity of the cell membrane in the presence of the SERS active substrate and at least suggesting that the changes in the vibrational spectra are not due to significant hemoglobin denaturation. Furthermore, the observed SERS spectra were used to distinguish submembrane hemoglobin from free unbound cytosolic hemoglobin due to the distance dependence of SERS.[25] Similar analysis will be carried out subsequently for RBCs on our substrates at this electronically nonresonant excitation wavelength.

With respect to the origin of the hypoxanthine signal in blood, no hypoxanthine vibrational bands are seen in the SERS spectrum of RBCs (Figure 6), and furthermore, no appreciable hypoxanthine vibrational features are observed in the SERS spectra of RBCs that have been stored in PBS or saline solution at 8 °C for 24 h (not shown). The dependence of the RBC SERS spectrum as a function of storage time in plasma will be the subject of a future study.

Significance of Hypoxanthine Signal. Hypoxanthine is a well-known, ubiquitous metabolite that is produced in the highly conserved purine degradation pathway found in both prokaryotic and eukaryotic cells. The nearly 100-fold increase of hypoxanthine in plasma of stored blood after 24 h was first noted more than 55 years ago via a procedure which involved deproteinization of the blood, conversion of hypoxanthine to uric acid by xanthine oxidase, and spectrophotometric determination of the uric acid concentration found by a UV absorption decrease following addition of the enzyme uricase.[56−58] Subsequently, techniques based on high-performance liquid chromatography following various procedures for deproteinization have been employed for determinations of hypoxanthine levels in whole blood or blood plasma.[59−65] The ability to accurately measure levels of hypoxanthine in blood or plasma is important for purine metabolism disorders such as xanthine oxidase deficiency,[59,66] hyperuricemia (gout),[67] and fetal hypoxia.[68] Elevated hypoxanthine has also been used in the early detection of acute cardiac ischemia[62,65] and may be a marker of prelabor fetal development problems.[64] The substitution of a SERS based methodology for detection of hypoxanthine and related small molecules offers advantages relative to HPLC approaches. First, SERS detection is fast, thus allowing essentially "real time" concentration measures to be determined for both rapid diagnostic capabilities and aiding fundamental studies of the biochemical mechanisms involving these species. Second, the SERS optical approach is easy to use. It requires minimal sample handling as compared to the HPLC approach. No deproteinization step is necessary, no additional chemical treatment steps are needed for detection, and no instrument calibration procedures, as required for HPLC-based identification techniques, have to be performed. Both chromatographic and SERS based techniques are inherently multiplexing detection schemes. Hypoxanthine and related compounds, such as adenine, adenosine, xanthine, inosine, and uric acid, are all strong SERS scatterers and can be spectrally distinguished. However, the sensitivity offered by SERS for hypoxanthine detection is as good, if not better, than that of HPLC. We have found that hypoxanthine in plasma can be detected at the ∼1 nM level, which appears to be more than an order of magnitude lower than that reported for HPLC methods.[62,63,66] Thus, SERS should provide a potentially valuable substitute for HPLC-based methods for the detection, identification, and quantification of purine compounds in blood or blood plasma for a variety of medical applications.

■ CONCLUSIONS

SERS spectra of whole human blood, plasma, and RBCs excited at 785 nm are reported for the first time and reveal a number of effects that are relevant to potential biomedical applications. In contrast to the normal Raman spectrum of whole blood, which is dominated by transitions to vibrational modes of hemoglobin, the SERS spectrum of fresh whole blood is only due to blood plasma when the sample preparation procedure employed here is followed. When a thin layer of whole blood is allowed to dry on our *in situ* grown Au nanoparticle covered

SiO_2 substrates, a SERS spectrum due to the proteins, lipoproteins, carbohydrates, and other small molecules including metabolites that are found in blood plasma is observed. For this sample preparation procedure, no cellular components of blood (RBCs, white blood cells, or platelets) contribute to the SERS spectrum of whole blood excited at 785 nm. Other methods for bringing this biological complex mixture into contact with metal nanoparticles, such as the more traditional Ag or Au nanoparticle colloid mixtures, as previously employed at 514 nm excitation,[24] may yield different SERS spectra of whole blood at this excitation wavelength (785 nm). The whole blood spectra due to these types of SERS media, as well as the Ag version of the sol−gel based Au substrates,[36] will be contrasted with the whole blood SERS results described here in subsequent work.

Excellent signal/noise SERS spectra of RBCs are obtained on the Au nanoparticle covered substrates excited at 785 nm, as shown here, and are the first reported at this excitation wavelength. Some vibrational bands are readily assignable to hemoglobin. The hemoglobin parentage of other slightly perturbed bands appear clear as well. However, the vibrational assignment of additional robust vibrational bands in this spectrum, which may be due to red blood cell membrane components or denaturation products, is outside the scope of this initial study and will be addressed in detail in following studies.

The time dependence of the SERS spectra of whole blood is probably the most significant biological result reported here. The SERS spectrum of whole blood becomes dominated by the vibrational signature of hypoxanthine within ∼24 h as a function of blood storage time after collection. The concentration of hypoxanthine is found to increase from the μM level to the several hundred μM level rather suddenly after ∼15 h, at least for the two donor blood samples described here. This component, and hence this biological activity, is not evident in the normal Raman spectrum excited at 785 nm. First, this speaks to the importance of using fresh human blood most generally for analytical probes of blood for disease detection and monitoring. Second, several studies employing 785 nm SERS spectra of serum for detection of different diseases, such as colorectal cancer,[5] diabetes,[26] nasopharyngeal cancer,[3] and gastric cancer,[4] have appeared very recently. The strongest vibrational band of the hypoxanthine at 724 cm^{-1} is evident in these SERS spectra. It is misidentified as adenine or coenzyme A and used as a disease marker in these multivariate data analysis based detection procedures. Knowledge of the time dependence of this hypoxanthine signature is critical for the accurate evaluation of the potential of such SERS based detection schemes and underscores the importance of understanding the chemical origins of hypoxanthine in this complex biological fluid. Subsequent studies must also determine the variability of the hypoxanthine rate of release in the population as a whole and for a given individual. In addition to the clinical applications, the time dependence of the hypoxanthine contribution to the SERS spectrum of human blood may be exploited as an age marker for forensic purposes, aside from the overall sensitivity enhancement that SERS detection provides.

In order to determine which of the cellular components account for the observed dramatic increase in hypoxanthine in stored blood, we will follow the time course of the SERS signals from RBCs, polymorphonuclear leukocytes, mononuclear leukocytes, and platelets in plasma. Identifying the particle or particles releasing hypoxanthine in blood and following its time course and magnitude via SERS in response to different stimuli will be useful for developing a molecular level understanding of the biochemical mechanism responsible for this dramatic effect. As described above, SERS would make a very attractive alternative to HPLC-based methods for monitoring purine compounds, including hypoxanthine, for the detection and study of a number of diseases or conditions such as xanthine oxidase deficiency, hyperuricemia, fetal hypoxia, fetal development problems, and, perhaps most significantly, ischemic heart disease.

■ ASSOCIATED CONTENT

Supporting Information

An SEM image of a typical Au nanostructured substrate used to acquire the SERS spectra described in this study (Figure S1). This material is available free of charge via the Internet at http://pubs.acs.org.

■ AUTHOR INFORMATION

Notes

The authors declare no competing financial interest.

■ ACKNOWLEDGMENTS

The support of the National Institute of Health (Grant # 1R01AI090815) is gratefully acknowledged.

■ REFERENCES

(1) Berger, A. J.; Itzkan, I.; Feld, M. S. *Spectrochim. Acta, Part A* **1997**, *53*, 287−292.
(2) Lyandres, O.; Shah, N. C.; Yonzon, C. R.; Walsh, J. T., Jr.; Glucksberg, M. R.; Van Duyne, R. P. *Anal. Chem.* **2005**, *77* (19), 6134−9.
(3) Feng, S.; Chen, R.; Lin, J.; Pan, J.; Chen, G.; Li, Y.; Cheng, M.; Huang, Z.; Chen, J.; Zeng, H. *Biosens. Bioelectron.* **2010**, *25* (11), 2414−9.
(4) Feng, S. Y.; Pan, J.; Wu, Y.; Lin, D.; Chen, Y.; Xi, G.; Lin, J.; Chen, R. *Sci. China Life Sci.* **2011**, *54*, 828−834.
(5) Lin, D.; Feng, S.; Pan, J.; Chen, Y.; Lin, J.; Chen, G.; Xie, S.; Zeng, H.; Chen, R. *Opt. Express* **2011**, *19* (14), 13565−77.
(6) Lin, J.; Chen, R.; Feng, S.; Pan, J.; Li, B.; Chen, G.; Lin, S.; Li, C.; Sun, L.-q.; Huang, Z.; Zeng, H. *J. Raman Spectrosc.* **2011**, *43*, 497−502.
(7) Harris, A. T.; Lungari, A.; Needham, C. J.; Smith, S. L.; Lones, M. A.; Fisher, S. E.; Yang, X. B.; Cooper, N.; Kirkham, J.; Smith, D. A.; Martin-Hirsch, D. P.; High, A. S. *Head Neck Oncol.* **2009**, *1*, 34.
(8) Hanlon, E. B.; Manoharan, R.; Koo, T. W.; Shafer, K. E.; Motz, J. T.; Fitzmaurice, M.; Kramer, J. R.; Itzkan, I.; Dasari, R. R.; Feld, M. S. *Phys. Med. Biol.* **2000**, *45* (2), R1−59.
(9) Hoey, S.; Brown, D. H.; McConnell, A. A.; Smith, W. E.; Marabani, M.; Sturrock, R. D. *J. Inorg. Biochem.* **1988**, *34* (3), 189−99.
(10) Carmona, P.; Monleon, E.; Monzon, M.; Badiola, J. J.; Monreal, J. *Raman Analysis of Prion Protein in Blood Cell Membranes from Naturally Affected Scrapie Sheep*; Cell Press: Cambridge, MA, ETATS-UNIS, 2004; Vol. *11*, p 6.
(11) Alvarez-Puebla, R. A.; Agarwal, A.; Manna, P.; Khanal, B. P.; Aldeanueva-Potel, P.; Carbo-Argibay, E.; Pazos-Perez, N.; Vigderman, L.; Zubarev, E. R.; Kotov, N. A.; Liz-Marzan, L. M. *Proc. Natl. Acad. Sci. U. S. A.* **2011**, *108* (20), 8157−61.
(12) Rusciano, G.; De Luca, A. C.; Pesce, G.; Sasso, A. *Sensors* **2008**, *8*, 7818−7832.
(13) Wood, B. R.; Stoddart, P. R.; McNaught, D. *Aust. J. Chem.* **2011**, *64*, 593−599.
(14) Berger, A. J.; Koo, T.-W.; Itzkan, I.; Horowitz, G.; Feld, M. S. *Appl. Opt.* **1999**, *38*, 2916−2916.
(15) Enejder, A. M. K.; Koo, T.-W.; Oh, J.; Hunter, M.; Sasic, S.; Feld, M. S. *Opt. Lett.* **2002**, *27*, 2004−2006.

(16) Stokes, R. J.; McBride, E.; Wilson, C. G.; Girkin, J. M.; Smith, W. E.; Graham, D. *Appl. Spectrosc.* **2008**, *62* (4), 371−6.
(17) Dieringer, J. A.; McFarland, A. D.; Shah, N. C.; Stuart, D. A.; Whitney, A. V.; Yonzon, C. R.; Young, M. A.; Zhang, X.; Van Duyne, R. P. *Faraday Discuss.* **2006**, *132*, 9−26.
(18) Camden, J. P.; Dieringer, J. A.; Zhao, J.; Van Duyne, R. P. *Acc. Chem. Res.* **2008**, *41* (12), 1653−61.
(19) Jeanmaire, D. L.; Van Duyne, R. P. *J. Electroanal. Chem.* **1977**, *84*, 1−20.
(20) Moskovits, M. *Rev. Mod. Phys.* **1985**, *57*, 783−826.
(21) Lombardi, J. R.; Birke, R. L. *J. Phys. Chem. C* **2008**, *112*, 5605−5617.
(22) Takahashi, M.; Niwa, M.; Ito, M. *J. Phys. Chem.* **1987**, *91* (1), 11−14.
(23) Fleger, Y.; Mastai, Y.; Rosenbluh, M.; Dressler, D. H. *Surf. Sci.* **2009**, *603*, 788−793.
(24) Casella, M.; Lucotti, A.; Tommasini, M.; Bedoni, M.; Forvi, E.; Gramatica, F.; Zerbi, G.; Spectrochim Acta, A. *Mol. Biomol. Spectrosc.* **2011**, *79* (5), 915−9.
(25) Brazhe, N. A.; Abdali, S.; Brazhe, A. R.; Luneva, O. G.; Bryzgalova, N. Y.; Parshina, E. Y.; Sosnovtseva, O. V.; Maksimov, G. V. *Biophys. J.* **2009**, *97* (12), 3206−14.
(26) Han, H. W.; Yan, X. L.; Dong, R. X.; Ban, G.; Li, K. *Appl. Phys. B: Lasers Opt.* **2009**, *94*, 667−672.
(27) Liu, R.; Zi, X.; Kang, Y.; Si, M.; Wu, Y. *J. Raman Spectrosc.* **2011**, *42*, 137−144.
(28) Kang, Y.; Si, M.; Liu, R.; Qiao, S. *J. Raman Spectrosc.* **2009**, *41*, 614−617.
(29) Smulevich, G.; Spiro, T. G. *J. Phys. Chem.* **1985**, *89*, 5168−5173.
(30) Xu, H.; Bjerneld, E. J.; Kall, M.; Borjesson, L. *Phys. Rev. Lett.* **1999**, *83*, 4357−4360.
(31) Virkler, K.; Lednev, I. K. *Anal. Bioanal. Chem.* **2010**, *396* (1), 525−34.
(32) Sikirzhytski, V.; Virkler, K.; Lednev, I. K. *Sensors* **2010**, *10*, 2869−2884.
(33) Premasiri, W. R.; Moir, D. T.; Klempner, M. S.; Krieger, N.; Jones, G., II; Ziegler, L. D. *J. Phys. Chem. B* **2005**, *109*, 312−320.
(34) Patel, I. S.; Premasiri, W. R.; Moir, D. T.; Ziegler, L. D. *J. Raman Spectrosc.* **2008**, *39* (11), 1660−1672.
(35) Premasiri, W. R.; Gebregziabher, Y.; Ziegler, L. D. *Appl. Spectrosc.* **2011**, *65* (5), 493−9.
(36) Premasiri, W. R.; Moir, D. T.; Klempner, M. S.; Ziegler, L. D. Surface enhanced Raman scattering of microorganisms. In *New Approaches in Biomedical Spectroscopy*; Kneipp, K., Aroca, R., Kneipp, H., Wentrup-Byrne, E., Eds.; Oxford University Press: New York, 2007; p 164.
(37) Zhang, J. Y.; Do, J.; Premasiri, W. R.; Ziegler, L. D.; Klapperich, C. M. *Lab Chip* **2010**, *10* (23), 3265−3270.
(38) Wood, B. R.; Tait, B.; McNaughton, D. *Biochim. Biophys. Acta* **2001**, *1539* (1−2), 58−70.
(39) Wood, B. R.; Caspers, P.; Puppels, G. J.; Pandiancherri, S.; McNaughton, D. *Anal. Bioanal. Chem.* **2007**, *387* (5), 1691−703.
(40) Venkatesh, B.; Ramasamy, S.; Mylrajan, M.; Asokan, R.; Manoharan, P. T.; Rifkind, J. M. *Spectrochim. Acta, Part A* **1999**, *55*, 1691−1697.
(41) Wood, B. R.; Hammer, L.; Davis, L.; McNaughton, D. *J. Biomed. Opt.* **2005**, *10* (1), 014005−13.
(42) Sato, H.; Chiba, H.; Tashiro, H.; Ozaki, Y. *J. Biomed. Opt.* **2001**, *6* (3), 366−70.
(43) Bankapur, A.; Zachariah, E.; Chidangil, S.; Valiathan, M.; Mathur, D. *PLoS One* **2010**, *5* (4), e10427.
(44) Karumuri, S. R.; Sekhar, J. V.; Sreeram, V.; Maheswara rao, V. U.; Basaveswara Rao, M. V. *J. Mol. Spectrosc.* **2011**, *269* (1), 119−123.
(45) Buschman, H. P.; Marple, E. T.; Wach, M. L.; Bennett, B.; Schut, T. C.; Bruining, H. A.; Bruschke, A. V.; van der Laarse, A.; Puppels, G. J. *Anal. Chem.* **2000**, *72* (16), 3771−5.
(46) Antonini, E.; Brunori, M. *Hemoglobin and Myoglobin in Their Reactions with Ligands*; North-Holland: Amsterdam, The Netherlands, 1971.
(47) Spiro, T. G. *Biological Applications of Raman Spectroscopy*; Wiley: New York, 1988; Vol. 3.
(48) Eaton, W. A.; Hanson, L. K.; Stephens, P. J.; Sutherland, J. C.; Dunn, J. B. R. *J. Am. Chem. Soc.* **1978**, *100*, 4991−5003.
(49) Zachariah, E.; Bankapur, A.; Santhosh, C.; Valiathan, M.; Mathur, D. *J. Photochem. Photobiol. B* **2010**, *100* (3), 113−6.
(50) Liu, R.; Zheng, L.; Matthews, D. L.; Satake, N.; Chan, J. W. *Appl. Phys. Lett.* **2011**, *99*, 043702−1−3.
(51) Shaklai, N.; Yguerabide, J.; Ranney, H. M. *Biochemistry* **1977**, *16* (25), 5585−92.
(52) Shaklai, N.; Yguerabide, J.; Ranney, H. M. *Biochemistry* **1977**, *16* (25), 5593−7.
(53) Garrett, R. H.; Grisham, C. M. *Biochemistry*, 4th ed.; Brooks/Cole: Boston, 2010.
(54) Spiro, T. G.; Strekas, T. C. *J. Am. Chem. Soc.* **1974**, *96* (2), 338−45.
(55) Wood, B. R.; McNaughton, D. *Biopolymers* **2002**, *67* (4−5), 259−62.
(56) Jorgensen, S.; Poulsen, H. E. *Acta Pharmacol. Toxicol.* **1955**, *11* (3), 223−43.
(57) Jorgensen, S. *Acta Pharmacol. Toxicol.* **1955**, *11*, 265−276.
(58) Jorgensen, S.; Poulsen, H. E. *Acta Pharmacol. Toxicol.* **1955**, *11* (3), 287−94.
(59) Boulieu, R.; Bory, C.; Baltassat, P.; Gonnet, C. *Anal. Biochem.* **1983**, *129* (2), 398−404.
(60) Kojima, T.; Nishina, T.; Kitamura, M.; Kamatani, N.; Nishioka, K. *Clin. Chem.* **1986**, *32*, 287−290.
(61) Harmsen, E.; de Jong, J. W.; Serruys, P. W. *Clin. Chim. Acta* **1981**, *115* (1), 73−84.
(62) Himmel, H. M.; Sadony, V.; Ravens, U. *J. Chromatogr.* **1991**, *568* (1), 105−15.
(63) Liu, Z.; Li, T.; Wang, E. *Analyst* **1995**, *120* (8), 2181−4.
(64) Sawa, R.; Yoneyama, Y.; Otsubo, Y.; Suzuki, S.; Kubonoya, K.; Power, G. G.; Araki, T. *J. Clin. Endocrinol. Metab.* **1997**, *82* (12), 4028−31.
(65) Farthing, D.; Sica, D.; Gehr, T.; Wilson, B.; Fakhry, I.; Larus, T.; Farthing, C.; Karnes, H. T.; Chromatogr, J.; Analyt Technol, B. *Biomed. Life Sci.* **2007**, *854* (1−2), 158−64.
(66) Boulieu, R.; Bory, C.; Baltassat, P.; Gonnet, C. *J. Chromatogr.* **1982**, *233*, 131−40.
(67) Yamamoto, T.; Moriwaki, Y.; Takahashi, S.; Nasako, Y.; Yamakita, J.; Hiroishi, K.; Higashino, K. *Anal. Biochem.* **1995**, *227* (1), 135−9.
(68) O'Connor, M. C.; Harkness, R. A.; Simmonds, R. J.; Hytten, F. E. *Br. J. Obstet. Gynaecol.* **1981**, *88* (4), 381−90.
(69) Abe, M.; Kitagawa, T.; Kyogoku, Y. *J. Chem. Phys.* **1978**, *69*, 4526−4534.
(70) Hu, S.; Smith, K. M.; Spiro, T. G. *J. Am. Chem. Soc.* **1996**, *118*, 12638−12646.